Heliyon 10 (2024) e33287

Contents lists available at ScienceDirect

Heliyon

journal homepage: www.cell.com/heliyon

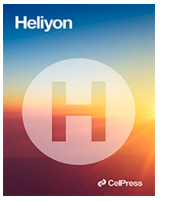

Research article

An "in control" hyaluronic acid nanogel with light-cleavable for rational use of antibiotics

Feifei Sun [a,b,c,*], Yao Xiao [c], Lili Kong [c], Haibo Mu [c], Xing Wang [c], Jinyou Duan [c,**]

[a] Key Laboratory of Systems Health Science of Zhejiang Province, School of Life Science, Hangzhou Institute for Advanced Study, University of Chinese Academy of Sciences, Hangzhou, 310024, China
[b] University of Chinese Academy of Sciences, China
[c] College of Chemistry & Pharmacy, Shaanxi Key Laboratory of Natural Products & Chemical Biology, Northwest A&F University, Yangling, Shaanxi, 712100, China

ARTICLE INFO

Keywords:
Hyaluronic acid
Nanogels
Light-responsive
Ciprofloxacin
Bacterial infection

ABSTRACT

The consequences caused by bacterial resistance are becoming more and more serious. The rate of antibiotic development is far behind the rate of bacterial resistance, so it is urgent to develop a new drug system. In this study, photoresponsive nanogels based on hyaluronic acid were prepared and loaded with ciprofloxacin as a model molecule. The results showed that the nanogels had the advantages of high stability and good cytocompatibility. The inhibition effect of drug-loaded nanogels after light irradiation on the growth of *Staphylococcus aureus* and *Salmonella typhimurium* was significantly better than that before light irradiation, and ciprofloxacin could be released on demand and in control. This strategy is of great significance to reduce the unnecessary use of antibiotics and weaken bacterial resistance.

1. Introduction

Hyaluronic acid (HA), a kind of natural anionic polysaccharide, also known as hyaluronan, is composed of repeated units of β-4 linked D-glucuronic acid and β-3 linked N-acetyl-D-glucosamine [1,2]. Because of many great characteristics, such as non-toxicity, biodegradability, cellular compatibility, non-immunogenic, and easy modification of structure, HA has been developed into a series of drug delivery systems, such as HA-modified liposomes, nano micelles, hydrogels, and so on ([3–5]; J. [6]; Z. [7]).

Bacterial infections are one of the world's most serious health problems, infecting millions of people every year [8]. The discovery and application of antibiotics ushered in a golden age of human safety: the ability to kill pathogenic microorganisms easily and easily. However, the improper overuse of antibiotics has led to the development of antibiotic resistance in bacteria. Yet new antibiotics are being developed far faster than bacteria can develop resistance. Due to the existence of resistance, traditional antibiotic treatments are often not effective in killing bacteria, which makes it urgent to find new treatment strategies. Drug delivery systems were born to address this challenge. It can precisely deliver the drug to the site of infection and achieve controlled release, increasing the local concentration of the drug, to kill bacteria more effectively. Therefore, it is of great practical significance to control the rational and

* Corresponding author. Key Laboratory of Systems Health Science of Zhejiang Province, School of Life Science, Hangzhou Institute for Advanced Study, University of Chinese Academy of Sciences, Hangzhou, 310024, China.
** Corresponding author. College of Chemistry & Pharmacy, Shaanxi Key Laboratory of Natural Products & Chemical Biology, Northwest A&F University, Yangling,Shaanxi, 712100, China.
E-mail addresses: sunfeifei@ucas.ac.cn (F. Sun), jduan@nwafu.edu.cn (J. Duan).

https://doi.org/10.1016/j.heliyon.2024.e33287
Received 1 March 2024; Received in revised form 15 June 2024; Accepted 18 June 2024
Available online 19 June 2024

effective use of existing antibiotics. Ciprofloxacin (CIP) is one of the third-generation quinolones widely used in clinical practice. Its main mechanism of action is to inhibit the activity of bacterial DNA rotase and interfere with the enzyme-catalyzed reaction to achieve the antibacterial effect (G.-F. [9]). It is a broad-spectrum antibiotic that is effective against most gram-negative bacteria and many gram-positive bacteria *in vitro*. The applications of smart drug delivery systems could release antibiotics on demand and in control and contribute to reducing their over-use [10,11].

Nanogels are a three-dimensional network system with high structural stability and good drug-loading capability formed by physical or chemical cross-linking of hydrophilic or amphiphilic polymers containing multi-functional groups [24]. As a multifunctional drug delivery system, nanogels are widely concerned for their small particle size, customizable synthesis, stable presence in blood circulation, and easy-to-load hydrophilic small-molecule drugs through core crosslinking. Besides, the introduction of response groups into the nanogels can make them respond in a specific environment, to realize the controllable and on-demand release of drugs [12–14]. For example, a kind of pH-responsive nanogels was reported to deliver protein for breast cancer in 2018 [15]. Nanogel is a kind of gel material with nanoscale size, which has high stability and controllability. The preparation of HA into nanogel can further develop its potential application in the biomedical field. On the one hand, the size effect of nanogels allows them to penetrate deeper into the skin or other biological tissues more easily, enabling more efficient drug delivery or therapeutic effects. On the other hand, the structural stability of the nanogel allows it to carry more drugs or active ingredients and control the speed and manner in which they are released, thereby improving treatment effectiveness and reducing side effects. The basic principle of using HA nanogels is to achieve more efficient and safer drug delivery and therapeutic effects by utilizing the biological properties of hyaluronic acid and the unique properties of the nanogels. In the field of medical cosmetology, HA nanogel can be used for skin moisturizing, wrinkle elimination, filling, etc., to restore the skin to a youthful state. In the field of drug delivery, hyaluronic acid nanogels can be used for targeted drug delivery, controlled release, etc., to improve the efficacy and safety of drugs.

Taking clues from the above, we hypothesized the nanogels could be prepared by light-cleavable HA derivatives with acrylamide groups and crosslinked by diethylene glycol diacrylate. Meanwhile, CIP could be loaded into the cavity of nanogels. Upon UV irradiation (365 nm), the “in control” HA nanogels underwent light cleavage, resulting in the release of CIP for the clearance of the pathogen.

Though a mass of drug delivery systems has been reported, antimicrobial delivery carriers are rare, especially for antibiotics at present. Using drug delivery systems could release antibiotics on demand, helping to reduce the overuse of antibiotics. So, in this paper, we convert HA into a light-responsive three-dimensional nanogel to deliver CIP which was employed as a model drug. Nuclear magnetic resonance spectrometer (NMR), Fourier transform infrared spectrometer (FTIR), UV–vis spectrophotometer, and dynamic light scatterer (DLS) were applied to analyze the physical and chemical characteristics of the HA-based nanogels. Besides the stability and cytotoxicity of the nanogels were also tested. The results showed that the nanogels could release CIP by irradiation and inhibit the growth of *Staphylococcus aureus* and *Salmonella typhimurium* effectively under light irradiation.

2. Materials and methods

2.1. Materials

Sodium hyaluronate (10 kDa) was purchased from QuFu GuangLong Biochem Co., Ltd. Tetrabutylammonium hydroxide (TBAH), 4-bromomethyl-3-nitrobenzoic acid (NB), thionyl chloride, N-(3-aminopropyl) methacrylamide hydrochloride (APMA·HCl) and N, N′-diisopropylethylamine (DIPEA) were purchased from Aladdin Chemical Reagent Company, China. 3-(4,5-dimethylthiazol-2-yl)-2,5-diphenyl tetrazolium bromide (MTT) and glutaraldehyde solution were obtained from Sigma Co. (St. Louis, MO, USA). Ion-exchange resin, Amberlite IR-120 was purchased from Alfa Aesar, China. Roswell Park Memorial Institute (RPMI) 1640 medium was purchased from Gibco Ltd. (Grand Island, NY, USA) and fetal bovine serum (FBS) was from Hyclone (Logan, UT, USA). Ciprofloxacin hydrochloride (HCl·Cipro), agar, and dialysis bag (10 kDa) were all purchased from Beijing Solarbio Science&Technology Co., Ltd. Dimethyl sulfoxide (DMSO) and other reagents were all of the analytical grades.

Staphylococcus aureus (MRSA, ATCC29213) and *Salmonella typhimurium* (SL1344) were generous gifts received from Prof. Xia (College of Food Science and Engineering, Northwest A&F University).

2.2. Synthesis of HA-NB-APMA

2.2.1. Synthesis of NB-Cl

NB-Cl was synthesized from NB and sulfoxide chloride as previously reported with minor modifications [16]. And the obtained product was directly used in the next step without purification.

2.2.2. Synthesis of NB-APMA

The freshly prepared NB-Cl was dissolved in 5 mL of anhydrous DCM, and the solution was added dropwise to an anhydrous DMF solution containing DIPEA (258 mg, 2.0 eq.) and APMA·HCl (170 mg, 1.2 eq.) in an ice bath. Then the reaction was stirred at 4 °C for 24 h and monitored by TLC. At the end of the reaction, the mixture was poured into distilled water and extracted with DCM. The DCM phase was separated and dried over Na_2SO_4 to obtain the crude product which was further separated and purified by silica gel column chromatography (petroleum ether: ethyl acetate = 4:1, *v/v*) to yield a colorless liquid (150 mg, 40 %). ^{1}H NMR (500 MHz, $CDCl_3$), δ (ppm): 8.62 (s, 1H), 8.17 (s, 1H), 8.02 (s, 1H), 7.79 (s, 1H), 6.39 (s, 1H), 5.79 (s, 1H), 5.37 (s, 1H), 4.97 (s, 2H), 3.52–3.48 (m, 2H), 3.47–3.44 (m, 2H), 2.00 (s, 3H), 1.78 (s, 2H).

2.2.3. Synthesis of HA-NB-APMA

HA-NB-APMA was synthesized according to a reported procedure with slight modifications ([17]; F. [18,19]). Sodium hyaluronate (10 kDa) was dissolved in distilled water and then passed through a cationicexchange resin (H^+ form). The above solution was neutralized by TBAH up to pH 7 obtaining HA salt named HA-TBAH. After freeze-drying, HA-TBAH (200 mg) was dissolved in anhydrous DMSO, followed by dropping above NB-APMA (10 mol% compared to the disaccharide units of HA) in dried DMSO. The mixture was stirred at 40 °C in the dark for 48 h, and dialysis was done against 0.1 M NaCl solution and distilled water respectively. Finally, the dialyzed solution was freeze-dried to obtain a cotton-like solid, which was designated as HA-NB-APMA.

2.3. Preparation of the HA-based nanogels

2.3.1. Preparation of HA-NB-APMA nanogels

To prepare the photo-cleavable HA-based nanogels, 50 mg of HA-NB-APMA and 63 mg of DEGDA were dissolved in 40 °C deionized water, then 100 mg of $K_2S_2O_8$ was added to the reaction after the system was heated to 70 °C under a nitrogen atmosphere. After the polymerization reaction had been initiated for 10 min, stopped heating and continued until the reaction system was cooled to room temperature. The HA nanogels were fabricated after the reaction mixture was dialyzed against a large amount of deionized water to remove monomers, initiators, cross-linking agents that did not participate in polymerization, and other impurities. We named the HA nanogels obtained after cross-linking HA-NB-APMA nanogels.

2.3.2. Preparation of the CIP-loaded HA-NB-APMA nanogels

Briefly, 1 mL of an aqueous solution of ciprofloxacin hydrochloride (HCl·CIP) was added dropwise to 5 mL of HA-NB-APMA nanogels dispersion (5 mg/mL). To neutralize the hydrochloric acid in HCl·CIP, the pH of the dispersion was adjusted to 8–9 by NaOH solution in advance and titrated to a final pH of 7.4. The mixture was stirred vigorously in the dark at room temperature for 16 h. Before use, the mixture was centrifuged at 15,000 rpm for 10 min to remove free CIP. Besides, the supernatant was collected and the precipitate was redispersed in a PBS solution at pH 7.4. Repeat the above process 3 to 5 times until the ideal state is gotten. The supernatant was collected and the concentration of CIP was measured by a UV–vis spectrophotometer at 270 nm. The drug loading content (DLC) and drug loading efficiency (DLE) were calculated according to the following formula:

DLC (wt.%) = (weight of loaded drug/total weight of loaded drug and polymer) × 100 %

DLE (%) = (weight of loaded drug/weight of the drug in feed) × 100 %

2.4. Characterization

2.4.1. Nuclear magnetic resonance (NMR) analysis

Nuclear magnetic resonance spectroscopy (^{1}H NMR) was measured on a Bruker AM 500 spectrometer concerning the chemical shift of the solvent peak. 5 mg of NB-APMA was weighed and dissolved in 600 μL of deuterated chloroform ($CDCl_3$), and 7 mg of HA-NB-APMA was dissolved in 600 μL of deuterated water (D_2O) to measure the corresponding ^{1}H NMR spectra.

2.4.2. FTIR analysis

The FTIR spectrum was determined using an FTIR spectrophotometer (BRUKER TEMSOR 27, BRUCK, Germany). The samples were grounded with KBr powder and pressed into a 1 mm pellet between 400 cm^{-1} and 4000 cm^{-1}.

2.4.3. Determination of critical micelle concentration (CMC)

To ensure the micelle formation and calculate the CMC of the amphiphilic molecule, the Nile red (NR), a hydrophobic fluorescence probe, was used to be loaded into the HA-NB-APMA or HA-NB-APMA nanogels [20]. The CMC was determined as previously reported [23] with minor modifications. Briefly, NR was loaded into different concentrations of HA-NB-APMA or HA-NB-APMA nanogels, and the fluorescence intensities of NR were measured by fluorospectro photometer at the emission wavelength of 550 nm.

2.4.4. Stability test

The stability of HA-NB-APMA nanogels was tested by loading NR into the core of HA-NB-APMA nanogels. Namely, NR-loaded HA-NB-APMA nanogels were put at different temperatures (4 °C and 37 °C). The fluorescence intensity of NR was measured and recorded.

2.4.5. Light-responsive test

2.4.5.1. The release profile of HA-NB-APMA nanogels. NR-loaded nanogels were put into a quartz tube and irradiated by UV light for a specific time. The fluorescence intensity of NR was recorded to show the light-responsiveness of HA-NB-APMA nanogels.

2.4.5.2. The changes of blank nanogels upon light irradiation. The blank HA-NB-APMA nanogels were placed into a quartz tube and irradiated by light for a different time. The UV–vis spectra were recorded.

2.4.6. Scanning electron microscopy (SEM)

The samples were dropped on the silicon wafers and dried at room temperature. The wafers were put on the sample stage and gold-

covered for SEM observations.

2.5. Cell, bacterial strains, and growth conditions

2.5.1. Bacterial strains

Staphyloccocus aureus (ATCC 29213), and *Salmonella typhimurium* (SL1344) were a kind of gift from Prof Xia.

2.5.2. Growth conditions

The two strains were cultured in Tryptic Soy Broth (TSB) at 37 °C. Active cultures were obtained by transferring loop cells from the TSB agar slant to a flask. Then they were incubated at 37 °C to the logarithmic phase of growth. After the OD of cell suspensions was adjusted to 0.4 at 600 nm, follow-up experiments could be carried out.

2.5.3. Cell culture

The spontaneously immortalized human keratinocytes (HaCat) cells were cultured in high glucose DMEM medium supplemented with 10 % FBS (fetal bovine serum), 100 U/mL penicillin, and 100 μg/mL streptomycin at 37 °C, 5 % CO_2. The cells were trypsinized using trypsin/EDTA when the cells reached approximately 80 % confluence.

2.6. Antibacterial assay

2.6.1. The preparation of light-responsive nanogels

The CIP-loaded HA-NB-APMA nanogels were irradiated by UV light (365 nm) for 4 h in the quartz tube, designated as CIP-loaded NGs UV-4 h.

2.6.2. The effect of CIP-loaded nanogels on the growth curve of bacteria

1.8 mL bacterial suspension (2×10^5 CFU/mL) was mixed with 0.2 mL nanomedicine or PBS as control and then was incubated in the shaker (37 °C, 120 rpm). The $OD_{600\ nm}$ was recorded at every hour.

2.6.3. The surface morphology observations of Staphyloccocus aureus

900 μL bacterial suspension (2×10^5 CFU/mL) was cultured on the cover glass in a 24-well plate, and the 100 μL nanomedicine or PBS was injected. After being incubated for 10 h, the supernatant was discarded. The cells were washed with PBS three times and fixed with GTA at 4 °C for 24 h. Next, the cells were dehydrated by 10 %, 30 %, 50 %, 70 %, 80 %, 90 %, and 100 % ethanol, respectively. After critically drying overnight with CO_2, the cover glasses were gold-covered by cathodic spraying for SEM observations.

2.7. Hemolysis assay

2.7.1 Female Kunming mice were used in this study; Mice handling and procedures were guided and approved by the Northwest A&F University Animal Care Committee (NWAFU-314020038); the male mice were not chosen because they are often aggressive and could cause damage to the cage mate and the sex of animals do not affect the experimental results. The mouse holding rooms were kept at 21 °C and 50 % relative humidity. All animal experiment procedures have been ethically reviewed and approved by the animal ethics committee of Northwest A&F University and complied with the National Research Council's Guide for the Care and Use of Laboratory Animals. The red blood cells (RBC) were collected from the mice (18–22 g) and were washed with saline solution several times. The concentration of the RBC was adjusted to 2 % by saline solution.

0.2 mL RBC solution mentioned above was dispersed in the tested solution (0.8 mL). Deionized water and PBS were used as the positive control (PC) and negative control (NC), respectively. After 2 h incubation at 37 °C, the samples were centrifuged at 6000 rpm for 5 min. The supernatant was removed and the optical density was recorded at 570 nm by a microplate reader. The hemolytic degree was calculated as follows:

$$\text{Hemolysis degree } (\%) = \frac{OD_{sample}\text{-}OD_{NC}}{OD_{PC}\text{-}OD_{NC}} \times 100$$

2.8. Cytotoxicity assay

The cytotoxicity of nanomedicine was tested on HaCat cells. Briefly, HaCat cells were seeded at a density of 2×10^4 cells per well in a 96-well plate and incubated at 37 °C in a 5 % CO_2 atmosphere for 4 h. The high glucose DMEM medium was discarded, and the cells were exposed to concentrations of samples varying from 200, 100, 50, and 25 μg/mL respectively. PBS was used as a blank control. After incubation for 24 h or 48 h, media were replaced with a fresh culture medium containing 10 μL MTT stock solution (5 mg/mL) to a total volume of 100 μL and further incubated for 4 h. Then, the plate was centrifuged for 5 min at 3500 rpm, and the supernatants were aspirated. The formazan crystals in each well were dissolved in 200 μL DMSO. After shaking for 10 min, the optical density of each well at 490 nm was measured by a microplate reader. Cell viability was evaluated in comparison to the control culture (taken as 100 %).

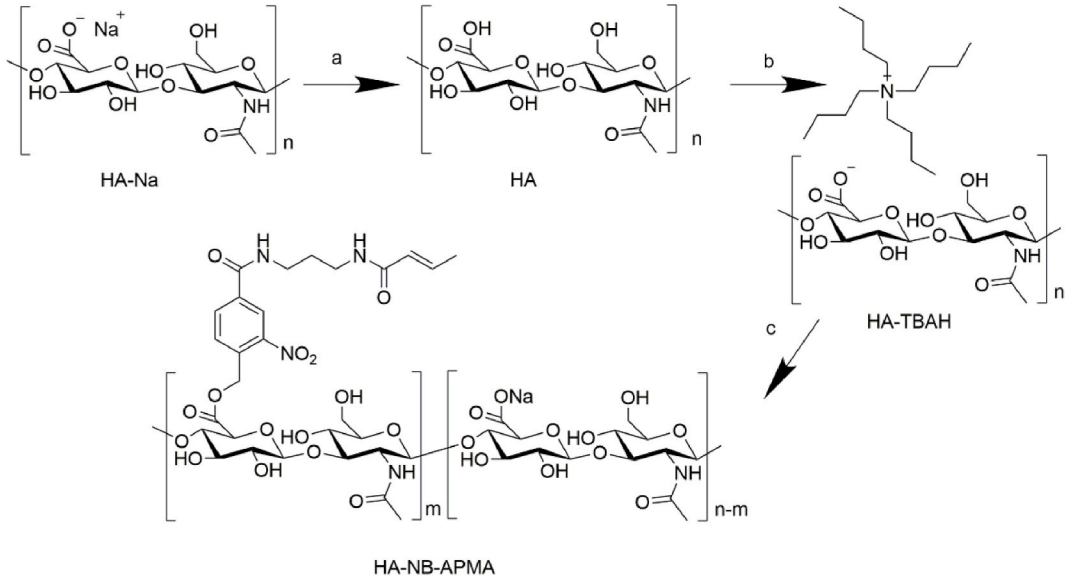

Fig. 1. The synthesis route of the amphiphilic molecule HA-NB-APMA. The commercial sodium hyaluronate solution (10 kDa, 5 mg/mL) was passed through a cationic-exchange resin (H+ form); b, the obtained hyaluronic acid solution was neutralized by an alkaline solution, TBAH; c, the lyophilized HA-TBAH was re-dissolved in dry DMSO and reacted with NB-APMA for 48 h at 40 °C.

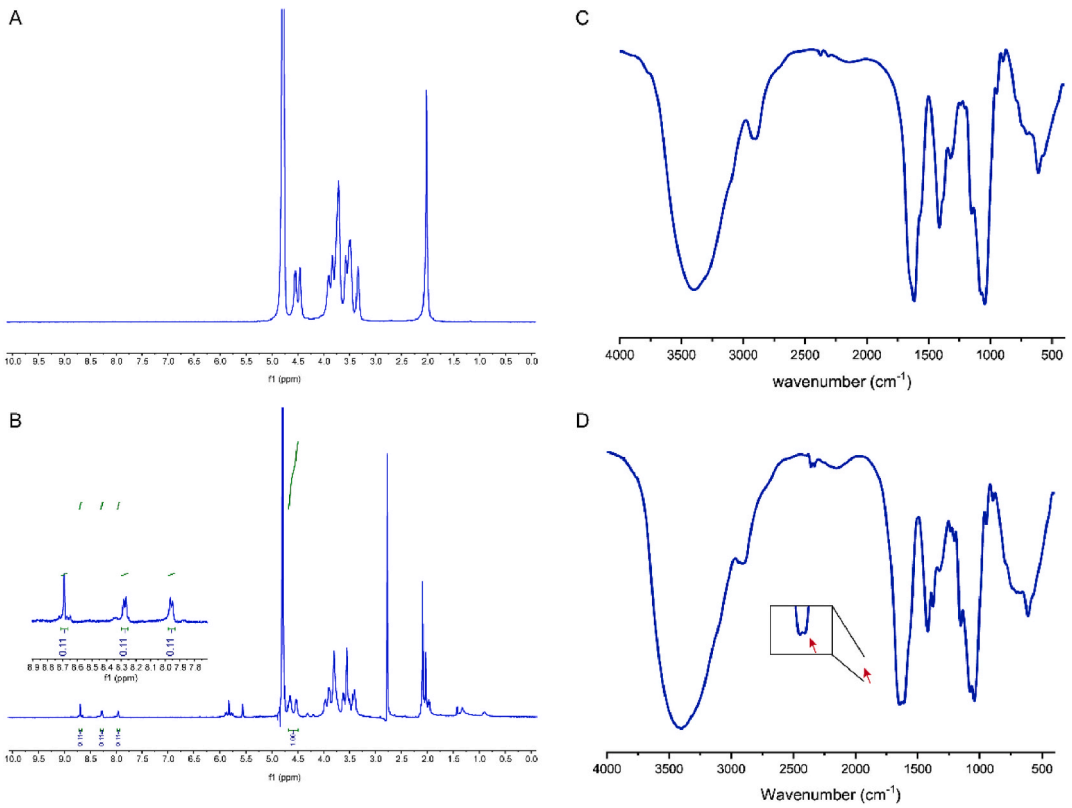

Fig. 2. The structural characterization of HA-NB-APMA. (A) The ^{1}H NMR spectrum of commercial HA; (B) The ^{1}H NMR spectrum of HA-NB-APMA obtained; (C) the FTIR spectra of HA (C) and HA-NB-APMA nanogels with fractionated gain (D).

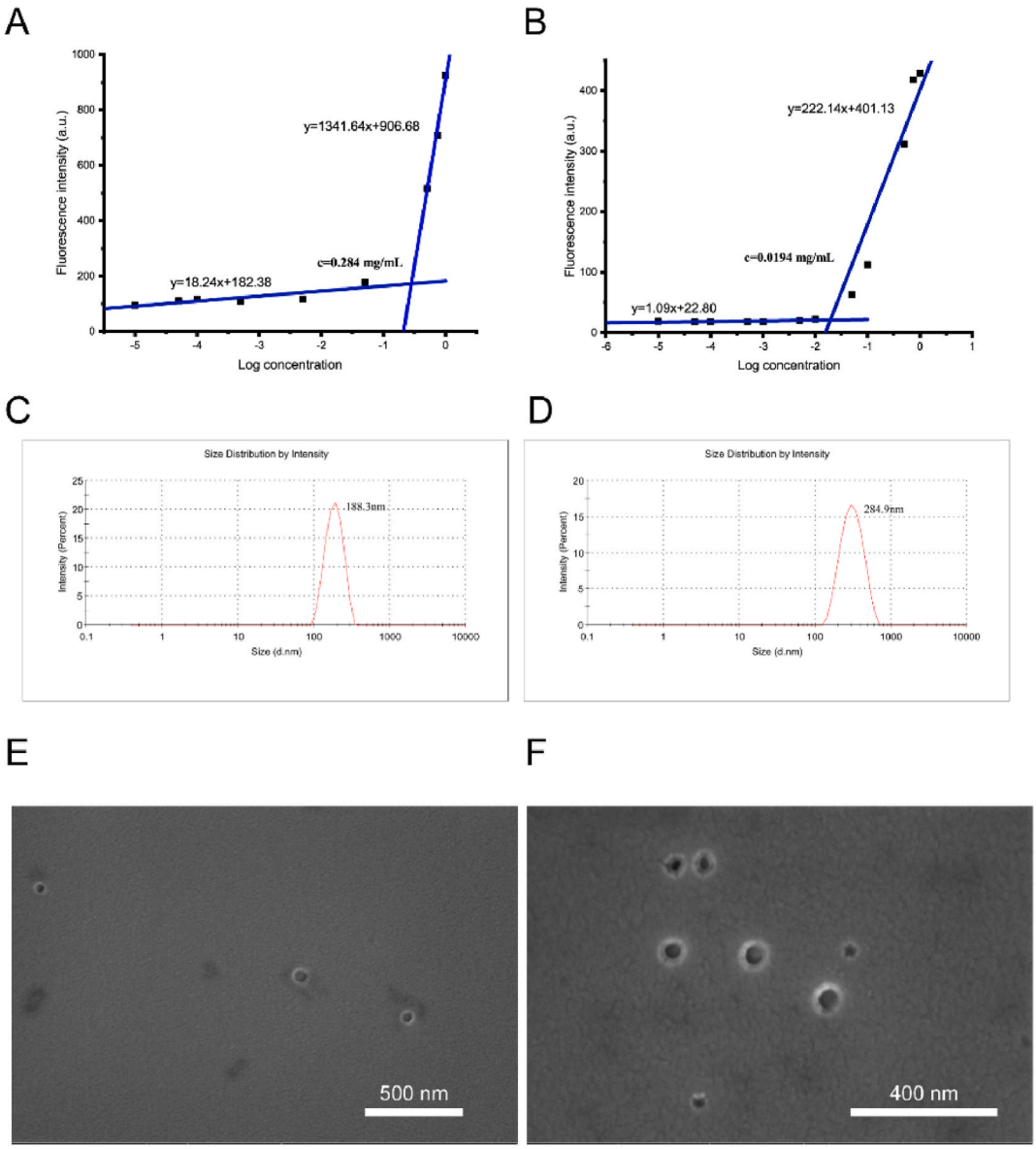

Fig. 3. The physical properties characterization of the HA-NB-APMA. The CMC values (A–B), size distributions (C–D), and SEM pictures (E–F) of the HA-NB-APMA before and after cross-linking, respectively.

2.9. Apoptosis assay

For the apoptosis assay, the HaCat cells were collected and seeded in the 12-well plate at the density of 5×10^4 cells per well; and after 4 h incubation at 37 °C in a 5 % CO_2 atmosphere, the corresponding nanogels at different concentrations were injected into the culture medium, respectively. The PBS was used as a blank control. After being incubated for 24 h, the cells were collected and treated as the instructions for the use of the kit. Finally, the cells were analyzed by flow cytometry.

2.10. Statistical analysis

Results were expressed as mean ± SD. Data were analyzed by *t*-test with the scientific statistic software GraphPad Prism 7.00.

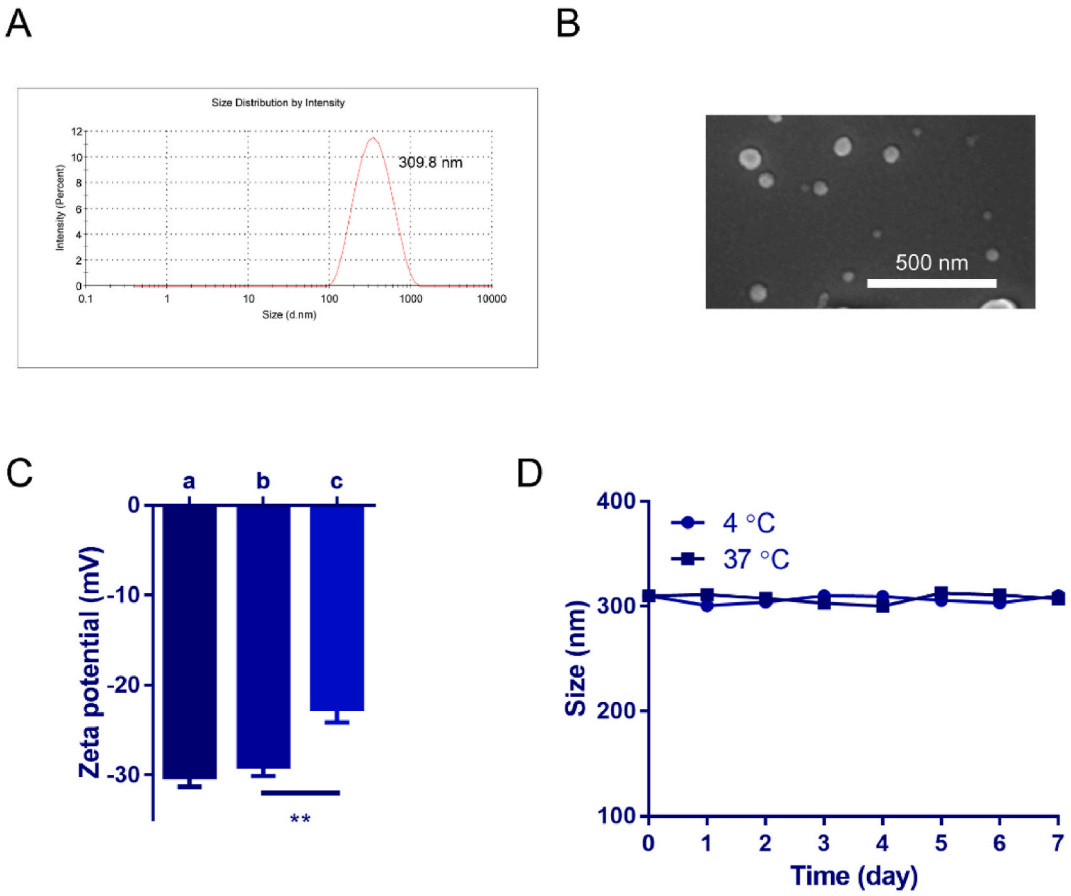

Fig. 4. The size distribution (A) and SEM picture of the CIP-loaded HA-NB-APMA nanogels. The zeta potentials of HA-NB-APMA (a), HA-NB-APMA nanogels (b), and CIP-loaded HA-NB-APMA nanogels (c). (D) The size changes of HA-NB-APMA nanogels at 4 °C and 37 °C from the stability test.

3. Results and discussion

3.1. Synthesis and characterization of HA-NB-APMA

To prepare the photoresponsive hyaluronic acid nanogels, it is necessary to introduce photoresponsive groups and double bonds into the HA backbone. For this purpose, the synthesis route was designed as shown in Figs. S1 and S2, and Fig. 1. First, NB reacted with $SOCl_2$ to form 4-bromomethyl-3-nitrobenzoyl chloride (NB–Cl). Then NB-Cl reacted with APMA·HCl to form NB-APMA, a lipid-soluble colorless liquid compound. Finally, an S_N1 nucleophilic substitution reaction occurred between NB-APMA and HA-TBAH in anhydrous DMSO.

The ^{1}H NMR spectra of HA and HA-NB-APMA were shown in Fig. 2. Compared with Fig. 2A (HA), some peaks appeared from 7.0 to 9.0 ppm in Fig. 2B, indicating the aromatic protons from the NB motif, which demonstrated the successful grafting of NB-APMA to HA. The N-acetyl protons for HA-NB-APMA and HA were assigned at 2.0 ppm. The esterification degree of free carboxyl acid in HA-NB-APMA was 7.33 %, according to the molar ratio of integration between N-acetyl and aromatic protons.

HA-NB-APMA obtained were amphiphilic molecules, which could self-assemble into micelles. So the CMC of HA-NB-APMA was measured by the method of NR as the fluorescent probe. As shown in Fig. 3A, the CMC of HA-NB-APMA was 0.284 mg/mL, suggesting poor stability.

3.2. Preparation and characterization of nanogels

The HA-based photo-responsive nanogels were acquired by the copolymerization between HA-NB-APMA and DEGDA, a kind of crosslinking agent containing carbon-carbon double bonds. From the FTIR spectrum of the nanogels in Fig. 2D, the absorption peak at 3400 cm^{-1} belongs to the -O-H from HA Fig. 2C; the peak at 1632 cm^{-1} belongs to the bending vibration peak of carbonyl groups. The information from the FTIR spectrum accounts for the successful synthesis of the nanogels, consistent with the literature (C. [21]). After copolymerization, the CMC dropped to 0.0194 mg/mL (Fig. 3B), namely, the process of copolymerization reduces CMC and improves the stability of the HA carrier. DLS results showed the sizes of HA-NB-APMA and nanogels were 188.3 and 284.9 nm, respectively; the

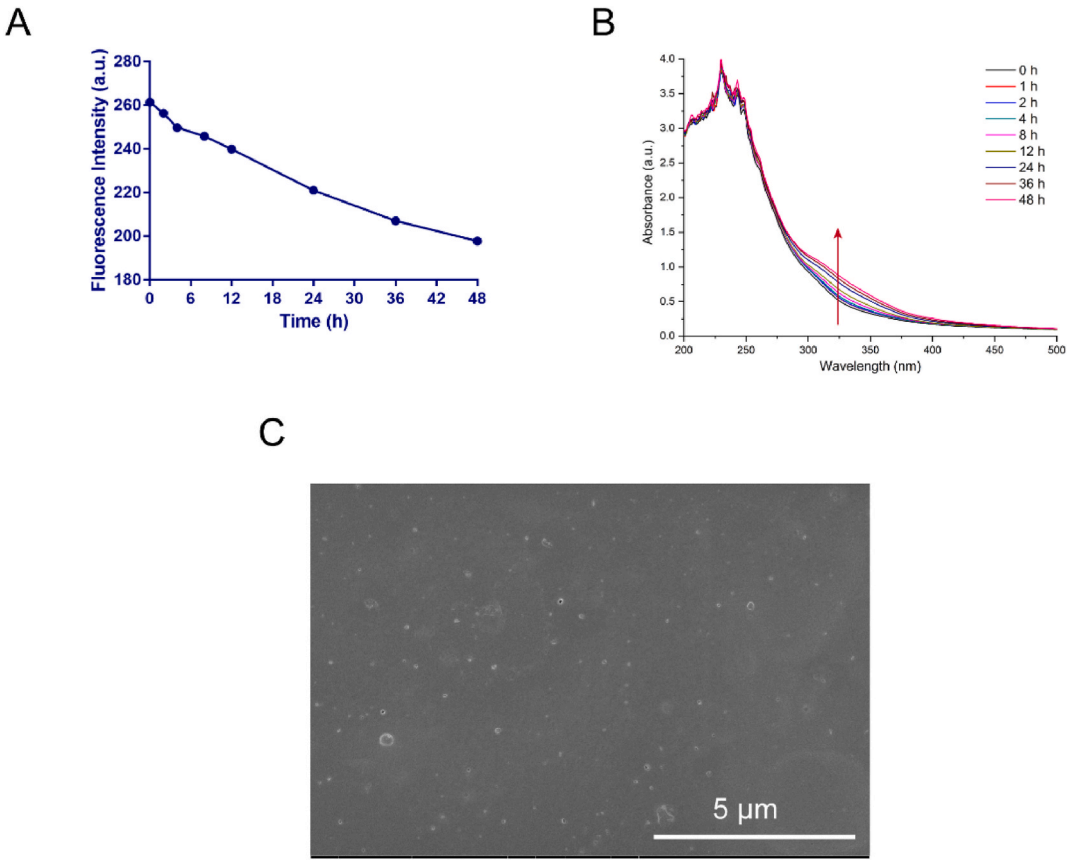

Fig. 5. (A) The NR release profile from the NR-loaded HA-NB-APMA nanogels upon the light irradiation. (B) UV–vis spectra of HA-NB-APMA solution irradiated for a different time. (C) The surface morphology of the HA-NB-APMA nanogels irradiated by UV light was pictured by SEM; the scale bar is 5 μm.

potentials were −30.23 and −29.2 mV, respectively. These results also indicate that copolymerization between HA-NB-APMA and DEGDA.

What's more, SEM was also used for analyzing the surface morphology (Fig. 3C ~ F). SEM pictures showed approximately spherical before and after copolymerization. The size was about 103 nm before copolymerization; it came to around 165 nm after copolymerization. These differ from the DLS results because the sample was in a liquid condition in DLS tests but solid-state in SEM observation.

Nanogels have cross-linked grid structures and strong water retention, so they could be developed as drug carriers for drug loading and delivery, especially for water-soluble drugs. In this paper, CIP was selected as the model drug, because it is the third generation of quinolones widely used in clinical practice with broad-spectrum antibacterial activity on *Staphylococcus aureus*, *Salmonella typhimurium*, *Pseudomonas aeruginosa*, *Escherichia coli,* and so on. The size and zeta potential of the HA nanogels were 309.8 nm showed in Fig. 4A and −22.63 mV after the drug loading showed in Fig. 4C, respectively. The SEM pictures in Fig. 4B showed approximately spherical. The DLC and DLE were 41.1 % and 69.7 %, respectively.

A qualified drug carrier should remain stable in different environments. So the nanogels were put at different temperatures (4 °C and 37 °C), and the size for blank nanogels and NR fluorescence intensity for NR-loaded nanogels based on HA was measured to express the stability. From Fig. 4D, there were no evident changes that happened in size distributions at both 4 °C for storage and 37 °C for the activity test. What's more, no obvious changes in fluorescence intensities in Fig. S4 were detected. The results mentioned have indicated the good stability of the nanogels. The zeta potentials were also recorded before and after cross-linking and drug-loading. It decreased after drug-loading quickly from −28 mV to −22 mV shown in Fig. 4D.

The potential clinical significance of the HA nanogel system is mainly reflected in its excellent drug delivery ability and therapeutic application. Due to the small size of nanogels, they could make it easier to achieve efficient drug delivery. HA-based nanogels have good dispersibility and can be better compatible with organisms, reducing adverse reactions such as immune rejection. At the same time, they also have a high drug delivery efficiency and can carry more drug molecules into the body. These properties make HA nanogels have a wide range of applications in drug delivery, therapeutic applications, tissue engineering, and sensor systems.

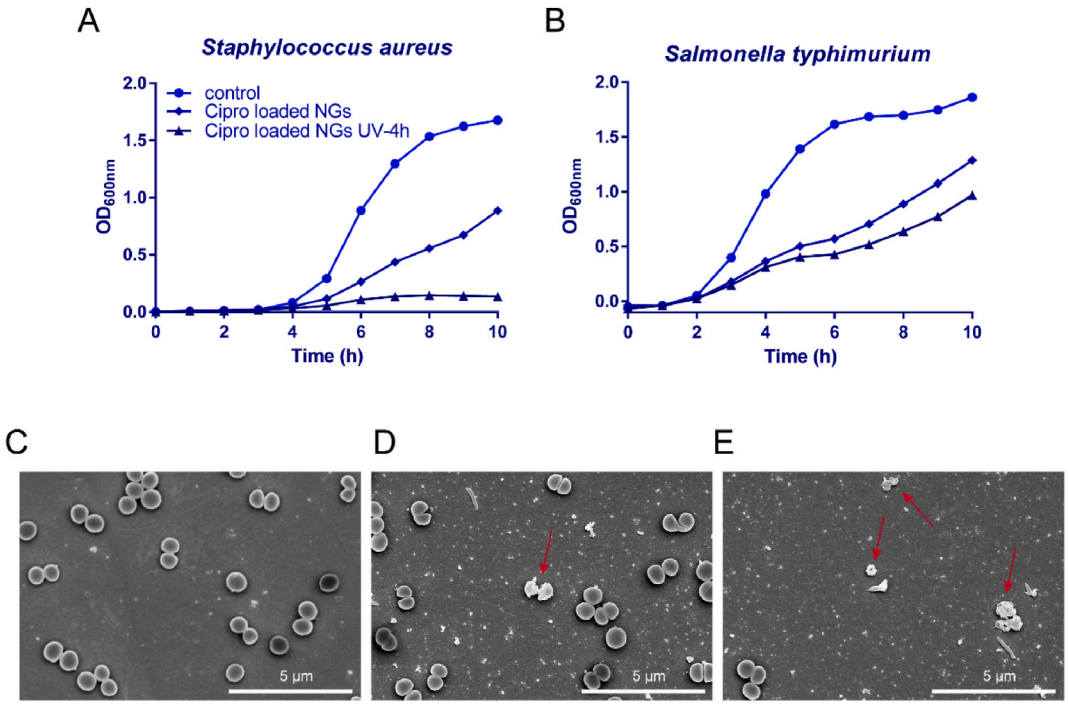

Fig. 6. The growth curves of *Staphylococcus aureus* (A) and *Salmonella typhimurium* (B) treated with different nanomedicine; and PBS was used as blank control. The bacteria morphology of *Staphylococcus aureus* treated by PBS (C), CIP-loaded HA-NB-APMA nanogels (D), and CIP-loaded HA-NB-APMA nanogels pretreated by light for 4 h (E); and PBS was used as blank control.

3.3. Response of the nanogels to light irradiation

The photo-triggered drug release experiment of nanogel was carried out by loading NR as a fluorescent molecule. The release curve as shown in Fig. 5A can be summarized that as the extension of irradiation time, the NR fluorescence intensity gradually reduces, showing that light irradiation broke the nitro–ortho ester bonds, disintegrated the nanogels system, released the NR molecules into the aqueous solution, reduced the solubility of NR in water, thus the fluorescence intensity of the detectable NR is reduced.

The UV–vis spectrophotometer was used to document the absorbance changes of the HA light-responsive nanogels upon photo-irradiation. The UV–vis absorption spectra were presented in Fig. 5B, from which the absorbance at 330 nm went up with the irradiation time extension, for the reason that the chemical bonds of the benzyl ester were broken, and the nitroso benzaldehyde derivative was produced when nanogels were irradiated by UV light. Also, on account of the rearrangement of aromatic π electrons involved, colored matters were produced and captured by a UV–vis spectrophotometer. The new peak indicated a non-localized aromatic system was generated, which was consistent with those reported in the literature [22].

The experimental results above revealed that the chemical bonds could be broken by light irradiation (365 nm), resulting in the fracture of the nanogels meshes. To get a better sense of the breakdown, the nanogels irradiated for 1 h were dropped onto the silicon wafer, dried, gold-covered, and observed by SEM. As shown in Fig. 5C, many small fragments were shot, which illustrated the disintegration of the nanogels.

3.4. Antibacterial effect of CIP-loaded nanogels

A kind of Gram-positive bacteria, *Staphylococcus aureus*, and a kind of Gram-negative bacteria, *Salmonella typhimurium*, were chosen to co-culture with CIP-loaded HA-NB-APMA nanogels or CIP-loaded HA-NB-APMA nanogels pre-treated by light. The growth curves were drawn by $OD_{600\ nm}$ *versus* time. As shown in Fig. 6A and B, though CIP-loaded nanogels could inhibit the growth of the two kinds of bacteria before and after light irradiation; the effect of CIP-loaded nanogels pre-treated by light irradiation on the pathogenic bacteria was better than the untreated nanogels. The reason for this phenomenon is that CIP-loaded nanogels pretreated by light irradiation in advance released part of CIP, which contained more free CIP to combat bacteria, thus achieving the effect of rapid inhibition of bacterial growth. In other words, the antibacterial effect of CIP-loaded nanogels pretreated by light was stronger than that without light treatment, indicating that the antibacterial effect of the HA-based nanogels loaded with CIP could be controlled by using light, thus realizing the purpose of releasing CIP at a fixed time and fixed point. This strategy of controlling the release of antibiotics helps to reduce the use of antibiotics and slow down the development of bacterial resistance.

To observe the antibacterial effect of the drug-loaded nano-gel visually, *Staphylococcus aureus* was selected as the observation object. In subsequent experiments, SEM was used to observe the bacterial morphology treated by CIP-loaded HA nanogels with or

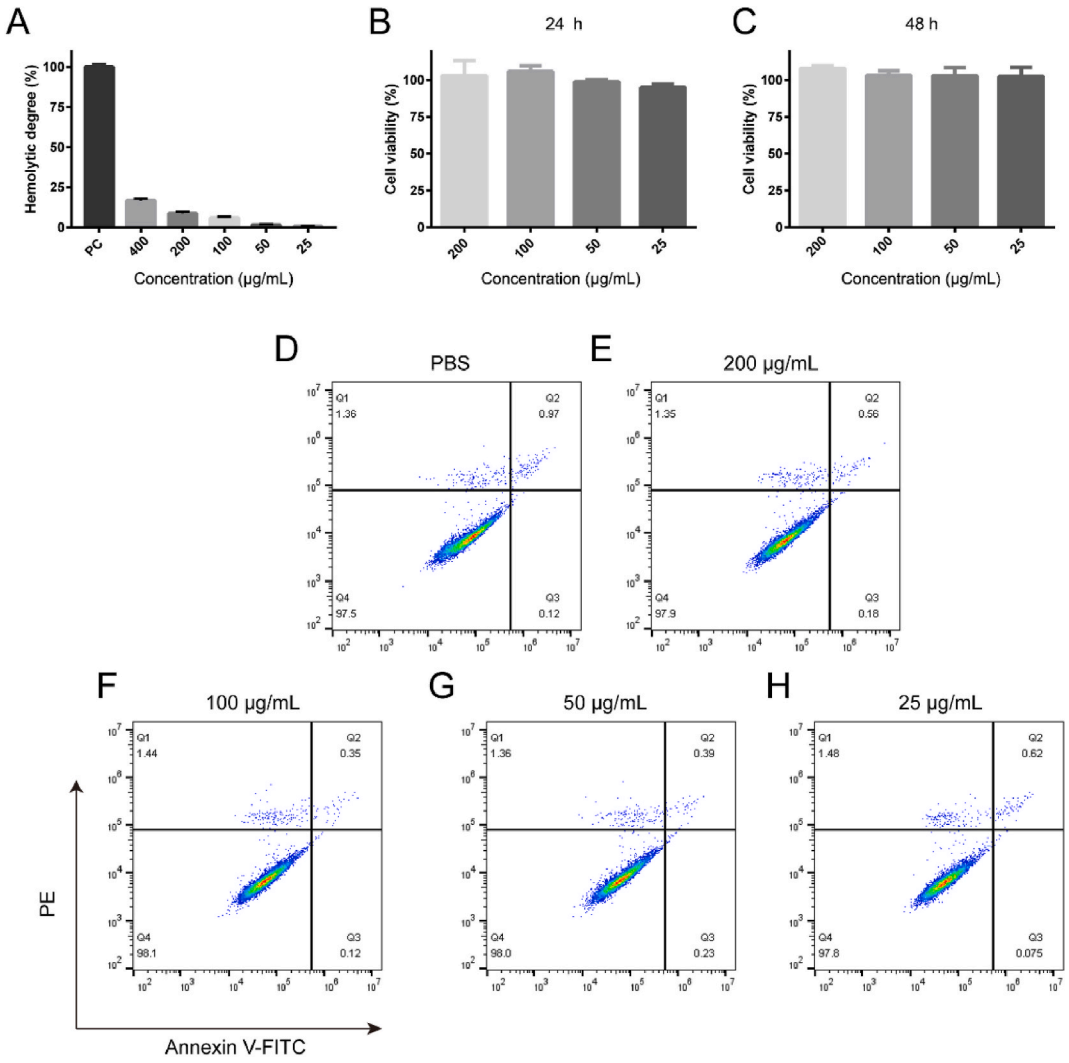

Fig. 7. The results of the biocompatibility of nanogels. (A) The evaluation of the blood compatibility of HA-NB-APMA nanogels. The cytotoxicity of HA-NB-APMA nanogels to HaCat cells for 24 h (B) and 48 h (C). The apoptosis ratio of HaCat cells treated by HA-NB-APMA nanogels for 24 h at various concentrations; and PBS was used as a blank control (D); E-H were the results of cells treated with 200, 100, 50, and 25 μg/mL, respectively.

without light pretreated for 10 h. The photos were shown in Fig. 6. Fig. 6C was the blank control group, that is, the bacteria in the normal states, it can be discovered that all the bacteria in this group showed uniform, round spherical; Fig. 6D showed the photo of bacteria treated by CIP-loaded HA nanogels. It can be observed that a few bacteria are broken, but most of them remain intact indicating the bacterial activity was still high. And Fig. 6E was the photo of bacteria exposed to CIP-loaded HA nanogels pretreated by light, only a few bacteria were observed in the picture. That was owing that the group contained a much higher concentration of free CIP, making the *staphylococcus aureus* reach more CIP, declining the vitality of bacteria. So, compared with other groups, these bacteria could not adhere to the cover glass, causing them were easy to be sucked away during the cleaning, fixation, dehydration, and other processes of the experiment. Only a few surviving bacteria or bacterial fragments were still stuck to the cover glass.

3.5. Biocompatibility of nanogels

That biocompatibility and biosafety are indispensable for biomaterials is widely recognized. The interaction of preparations with blood components is also of great requirement in pathophysiological events (Fig. 7A). The rate of hemolysis was around a safe margin for the nanogels based on HA over a wide range of concentrations from 400 to 25 μg/mL, revealing the good biocompatibility of HA-NB-APMA nanogels. Moreover, the toxicity of the HA nanogels on HaCat cells was evaluated by MTT colorimetric method, and the results are shown in Fig. 7B and C. It was shown that the cell viability of HaCat cells cocultured with different concentrations of HA nanogels (200, 100, 50, 25 μg/mL) for 24 or 48 h remained at about 100 %, indicating the good biocompatibility and safety of the HA nanogels. Finally, to assess the safety of the nanogels, the apoptosis of HaCat cells was measured shown in Fig. 7D–H. From the

apoptosis results, few cells showed apoptosis, namely, the majority of cells were alive and healthy. The results above demonstrated the great biocompatibility of HA-NB-APMA nanogels, which suggested the potential application of the nanogels based on HA at pathophysiological events.

4. Conclusions

In this paper, the HA-based nanogels with light responsiveness were prepared to deliver the quinolone antibiotic, CIP. The results revealed the high stability and good biocompatibility of the HA nanogels. The idea could potentially be used to treat patients with skin infections in the clinic to help them avoid developing antibiotic resistance. From the experiments in combating *Staphylococcus aureus* and *Salmonella typhimurium*, the inhibition effect of the drug-carrying nanogels treated with the light on the growth of the two kinds of bacteria was significantly better than that of the nanogels treated without light, achieving the controlled and on-demand release of CIP. In a word, the HA nanogels were an ideal antibiotic delivery system with potential application value, which provided a new idea for promoting the rational use of antibiotics and reducing the emergence of bacterial resistance.

Ethics statement

Mice handling and procedures were guided and approved by the Northwest A&F University Animal Care Committee (NWAFU-314020038).

CRediT authorship contribution statement

Feifei Sun: Writing – review & editing, Resources, Project administration, Funding acquisition, Data curation, Conceptualization. **Yao Xiao:** Writing – original draft, Visualization, Investigation. **Lili Kong:** Investigation. **Haibo Mu:** Validation. **Xing Wang:** Writing – original draft. **Jinyou Duan:** Writing – review & editing, Funding acquisition.

Declaration of competing interest

The authors declare that they have no known competing financial interests or personal relationships that could have appeared to influence the work reported in this paper.

Acknowledgments

This work was supported by the Research Funds of Hangzhou Institute for Advanced Study (2022ZZ01010) and the National Natural Science Foundation of China (NSFC) (31570799).

Appendix A. Supplementary data

Supplementary data to this article can be found online at https://doi.org/10.1016/j.heliyon.2024.e33287.

References

[1] B. Weissmann, K. Meyer, The structure of hyalobiuronic acid and of hyaluronic acid from umbilical Cord1,2, J. Am. Chem. Soc. 76 (7) (1954) 1753–1757.
[2] B. Weissmann, K. Meyer, P. Sampson, A. Linker, Isolation of oligosaccharides enzymatically produced from hyaluronic acid, J. Biol. Chem. 208 (1) (1954) 417–429.
[3] C. Lu, Y. Xiao, Y. Liu, F. Sun, Y. Qiu, H. Mu, J. Duan, Hyaluronic acid-based levofloxacin nanomicelles for nitric oxide-triggered drug delivery to treat bacterial infections, Carbohydr. Polym. 229 (2020) 115479.
[4] L. Mo, J.G. Song, H. Lee, M. Zhao, H.Y. Kim, Y.J. Lee, H.K. Han, PEGylated hyaluronic acid-coated liposome for enhanced in vivo efficacy of sorafenib via active tumor cell targeting and prolonged systemic exposure, Nanomedicine 14 (2) (2018) 557–567.
[5] N. Sahiner, S.S. Suner, R.S. Ayyala, Preparation of hyaluronic acid and copolymeric hyaluronic acid: sucrose particles as tunable antibiotic carriers, J. Polym. Res. 27 (7) (2020).
[6] J. Yang, Y. Liu, L. He, Q. Wang, L. Wang, T. Yuan, X. Zhang, Icariin conjugated hyaluronic acid/collagen hydrogel for osteochondral interface restoration, Acta Biomater. 74 (2018) 156–167.
[7] Z. Zhang, S.S. Suner, D.A. Blake, R.S. Ayyala, N. Sahiner, Antimicrobial activity and biocompatibility of slow-release hyaluronic acid-antibiotic conjugated particles, Int. J. Pharm. 576 (2020).
[8] S.Y. Tong, J.S. Davis, E. Eichenberger, T.L. Holland, V.G. Fowler Jr., Staphylococcus aureus infections: epidemiology, pathophysiology, clinical manifestations, and management, Clin. Microbiol. Rev. 28 (3) (2015) 603–661.
[9] G.-F. Zhang, X. Liu, S. Zhang, B. Pan, M.-L. Liu, Ciprofloxacin derivatives and their antibacterial activities, Eur. J. Med. Chem. 146 (2018) 599–612.
[10] E. Imbuluzqueta, C. Gamazo, J. Ariza, M.J. Blanco-Prieto, Drug delivery systems for potential treatment of intracellular bacterial infections, Frontiers in Bioscience-Landmark 15 (2) (2010) 397–417.
[11] H. Mu, H. Bai, F. Sun, Y. Liu, C. Lu, Y. Qiu, J. Duan, Pathogen-targeting glycovesicles as a therapy for salmonellosis, Nat. Commun. 10 (1) (2019) 4039.
[12] K.H. Bae, H. Mok, T.G. Park, Synthesis, characterization, and intracellular delivery of reducible heparin nanogels for apoptotic cell death, Biomaterials 29 (23) (2008) 3376–3383.
[13] J.K. Oh, D.J. Siegwart, K. Matyjaszewski, Synthesis and biodegradation of nanogels as delivery carriers for carbohydrate drugs, Biomacromolecules 8 (11) (2007) 3326–3331.

[14] N.A. Peppas, J.Z. Hilt, A. Khademhosseini, R. Langer, Hydrogels in biology and medicine: from molecular principles to bionanotechnology, Adv. Mater. 18 (11) (2006) 1345–1360.
[15] L. Ding, Y. Jiang, J. Zhang, H.A. Klok, Z. Zhong, pH-Sensitive coiled-coil peptide-cross-linked hyaluronic acid nanogels: synthesis and targeted intracellular protein delivery to CD44 positive cancer cells, Biomacromolecules 19 (2) (2018) 555–562.
[16] R. Wang, G. Zhu, L. Mei, Y. Xie, H. Ma, M. Ye, W. Tan, Automated modular synthesis of aptamer-drug conjugates for targeted drug delivery, J. Am. Chem. Soc. 136 (7) (2014) 2731–2734.
[17] S. Pelletier, P. Hubert, F. Lapicque, E. Payan, E. Dellacherie, Amphiphilic derivatives of sodium alginate and hyaluronate: synthesis and physico-chemical properties of aqueous dilute solutions, Carbohydr. Polym. 43 (4) (2000) 343–349.
[18] F. Sun, Y. Liu, D. Wang, Z. Wang, H. Mu, F. Wang, J. Duan, A novel photocleavable heparin derivative with light controllable anticoagulant activity, Carbohydr. Polym. 184 (2018) 191–198.
[19] C.P. Vázquez, T. Boudou, V. Dulong, C. Nicolas, C. Picart, K. Glinel, Variation of polyelectrolyte film stiffness by photo-cross-linking: a new way to control cell adhesion, Langmuir 25 (6) (2009) 3556–3563.
[20] D. Hu, H. Peng, Y.L. Niu, Y.F. Li, Y.C. Xia, L. Li, W.J. Xu, Reversibly light-responsive biodegradable poly(carbonate) micelles constructed via CuAAC reaction, J. Polym. Sci. Polym. Chem. 53 (6) (2015) 750–760.
[21] C. Yang, X. Wang, X. Yao, Y. Zhang, W. Wu, X. Jiang, Hyaluronic acid nanogels with enzyme-sensitive cross-linking group for drug delivery, J. Contr. Release 205 (2015) 206–217.
[22] P. Anilkumar, E. Gravel, I. Theodorou, K. Gombert, B. Theze, F. Duconge, E. Doris, Nanometric micelles with photo-triggered cytotoxicity, Adv. Funct. Mater. 24 (33) (2014) 5246–5252.
[23] F. Sun, P. Zhang, Y. Liu, C. Lu, Y. Qiu, H. Mu, J. Duan, A photo-controlled hyaluronan-based drug delivery nanosystem for cancer therapy, Carbohydr. Polym. 206 (2019) 309–318.
[24] Z. Zhang, G. Hao, C. Liu, J. Fu, D. Hu, J. Rong, X. Yang, Recent progress in the preparation, chemical interactions and applications of biocompatible polysaccharide-protein nanogel carriers, Food Res. Int. 147 (2021) 110564.